Rat Model of Induced Membrane Technique with an Autologous Iliac Bone Graft

Kanu Shimokawa[1], Hidenori Matsubara[1], Toshifumi Hikichi[1], Fushitani Yuki
[1]Kanazawa University

INTRODUCTION: The treatment of segmental bone defects and nonunions represents a major clinical challenge for orthopaedic surgeons. The induced membrane technique (IMT), also known as the Masquelet technique, is a two-stage surgical procedure that has gained popularity in the management of fracture nonunions and large bone defects. Despite the increased clinical application of IMT, several aspects of the technique are controversial. Several animal models have been developed to characterize IMT and test the effect of parameter variations on membrane formation and subsequent bone healing. However, there are few reports on IMT using autologous iliac bone grafts in rat models. Therefore, this study aimed to establish rat IMT models using autologous iliac cancellous bone (AICB) grafts.

METHODS:

We used healthy male Sprague-Dawley rats aged 12 weeks and weighing 350-400g. A skin incision was made over the right femur and an external fixator was fixed with four self-tapping pins in the femur (Figure 1a,b). Two osteotomies were performed between the second and third pins to create a 5-mm segmental defect. A polymethyl methacrylate spacer was placed in each defect (Figure 1c). The rats underwent a second surgery 2 weeks after the first. The spacer was removed, and the membranous chamber between the two bone ends was filled in three patterns: without implants (group A), with a block of β-TCP artificial bone (group B), and with AICB (group C).

Collection of AICB was performed as previously reported by our group, as follows: an approach was made through a vertical incision, approximately 4 cm long along the dorsal midline region (Figure 1d). The bilateral iliac crests were identified and harvested (Figure 1e). The cancellous bone of the iliac crest was separated from the cortical bone using a scalpel, and the crushed cancellous bone was compressed into a 5 mm block (Figure 1f,g).

Specimens were evaluated using digital image analysis, histology, and real-time reverse transcription polymerase chain reaction (RT-PCR). For radiographic evaluation, all femurs were evaluated using X-ray micro-computed tomography at 2, 4, 6, and 8 weeks after the second operation (n=15 per group). For histological analysis of the tissues, the femurs harvested at 2, 4, 6, and 8 weeks after the second operation. After dealing, the external fixator was removed and the specimens were sectioned in the sagittal plane, stained with hematoxylin and eosin (HE), and assessed using an optical microscope. For real-time RT-PCR analysis, tissue from the transplant site was harvested 4 weeks after the second operation, and RNA was extracted (n=5 per group). Glyceraldehyde-3-phosphate dehydrogenase (GAPDH), bone morphogenetic protein 2 (BMP-2), vascular endothelial growth factor (VEGF), and transforming growth factor beta (TGF-β) were assessed. The expression level of each target gene was calculated relative to that of GAPDH in each sample.

RESULTS:

HE staining of the membrane tissue collected 2 weeks after the first surgery revealed an inner layer with intensive fibrous tissue and an outer layer with loose connective tissue and microvessels (Figure 2a,b). This feature is consistent with previously reported pathology of the induced membrane.

On radiographic evaluation, the union rate at the transplantation site was 0% in Group A, 6.7% in Group B, and 66.7% in Group C (Figure 3). In histological evaluation, sagittal sections stained with HE 2 weeks after surgery showed that the grafted cancellous bone was located within the bone defect (Figure 2c,d). The grafted cancellous bone was converted into new bone over time. After 6 weeks, the chondrocyte layer nearly disappeared, and the new bone connected both the sides (Figure 2e-g). RT-PCR analysis revealed higher expression levels of BMP -2, TGF-β, and VEGF genes in group C than that in other groups (Figure 4).

DISCUSSION AND CONCLUSION:

IMT has become a popular technique for treating bone defects and nonunions. However, the best application of this technique in clinical settings remains debatable. Harvesting the graft material from the iliac crest is one of the most common clinical approaches. However, previously reported rat models have used allogeneic bone grafts, tail bone autografts, or artificial bones, with no reports using only AICB grafts. To the best of our knowledge, the IMT model reported herein is the first to use AICB grafts in rats. In this study, nonunion was observed in the group without bone grafts or with artificial bone grafts, and AICB grafts led to good bone union, indicating that AICB grafts strongly promoted bone union in rats.

In conclusion, we established a stable rat IMT model using AICB grafts by harvesting the iliac bone. This model can aid in further investigation of IMT and future development of novel therapies for bone injury.

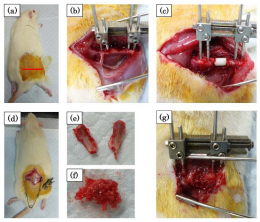

< Figure 1 >
(a) A skin incision was made over the right femur.
(b) An external fixator was fixed in the femur.
(c) 5-mm segmental defect was created and a polymethyl methacrylate spacer was placed in each defect.
(d) A skin incision was made along the dorsal midline region.
(e) the bilateral iliac crests and (f) the crushed cancellous bone
(g) A spacer was removed and the iliac cancellous bone was grafted.

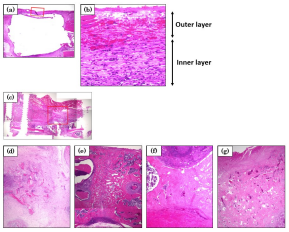

< Figure 2 >
HE staining of the membrane tissue collected 2 weeks after the first surgery revealed two layers construction (a: magnification × 2, b: magnification × 40).
HE staining of the grafted site at the point of 2, 4, 6, and 8 weeks after second surgery,(c: 2 weeks, magnification × 2, d: 2 weeks, magnification × 10, e: 4 weeks, magnification × 10, f: 6 weeks, magnification × 10, g: 8 weeks, magnification × 10).

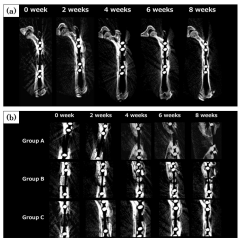

< Figure 3 >
(a) Computed tomography micrographs of the model rats of group C (autologous iliac cancellous bone) at sequential time points.
(b) Computed tomography micrographs of the model rats of group A, B, and C at sequential time points.

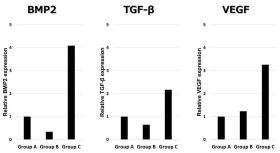

< Figure 4 >
Relative expression levels of BMP-2, TGF-ß, VEGF among the different of implantation using real time-PCR.